studied in this work with respect to covalent addition and electrochemical reduction reactions. In some further cases this different behavior may arise because of profound differences in the kinetics of the reactions as compared to those of the heterocyclic molecules that have been studied, but in other cases marked differences may exist between the structures of the most stable radicals and adducts, respectively. Studies are continuing in our laboratories to determine how widely applicable the correlation that has been discussed is to the prediction of covalent additions to heteroaromatic molecules.

Experimental Section

Quinazoline, acridine, purine, and pyrimidine were purchased from Aldrich Chemical Co. The other heterocyclic compounds were purchased from K & K Laboratories, Inc. These chemicals were used without further purification. All other chemicals were reagent or analytical grade.

Polarographic data were obtained with a Model 174 polarographic analyzer (Princeton Applied Research Corp., Princeton, N.J.) equipped with a model 174/70 drop timer. Polarographs were recorded on an Omnigraphic Model 2000 X-Y recorder (Houston Instrument Co., Austin, Texas). The dropping mercury electrode used had a flow rate $m = 3.2$ mg s^{-1} in deionized water at an uncorrected height of the mercury reservoir $h = 60$ cm and a natural drop time $t_\alpha = 2.1$ s in 0.1 M hydrogen chloride solution at -0.60 V vs. SCE. The cell was equipped with a saturated calomel reference electrode and graphite rod counter electrode. A purified nitrogen stream was used to deoxygenate the solutions. All measurements were carried out at room temperature. Measurements of pH were made with a Corning Model 112 expanded scale/digital pH meter. Buffer solutions in the range from pH 1.0 to 2.2 were prepared from 0.2 M HCl and 0.2 M KCl solutions. The compounds were dissolved in the desired buffer to give 5×10^{-5}–10^{-3} M solutions; the pH of each solution was measured. About 8 ml of test solution was transferred to the cell, purged with nitrogen for 10 min, and then polarographed. Gelatin (concentration 0.01%) was used in purine and adenine solutions to suppress maxima. A portion of the buffer solution was treated in identical fashion to obtain the background curve.

Equilibrium constants for bisulfite addition to purine and acridine were calculated from the results of similar experiments to those which have been described previously.[12] Ionic strength was maintained at 1.0 M with sodium chloride and the temperature was 25.0 ± 0.1 °C. Results are in Tables I and II.

References and Notes

(1) Supported in part by NIH grant No. R01-GM18348. I.H.P. is the holder of NIH Career Development Award No. K04-GM 70100.
(2) D. D. Perrin and I. H. Pitman, *J. Chem. Soc.*, 7071 (1965).
(3) R. Shapiro, R. E. Servis, and M. Welcher, *J. Am. Chem. Soc.*, **92**, 422 (1970).
(4) G. S. Rork and I. H. Pitman, *J. Am. Chem. Soc.*, **96**, 4654 (1974).
(5) G. S. Rork and I. H. Pitman, *J. Pharm. Sci.*, **64**, 216 (1975).
(6) F. A. Sedor, D. G. Jacobson, and E. G. Sander, *J. Am. Chem. Soc.*, **97**, 5572 (1975).
(7) R. Shapiro, B. I. Cohen, and R. E. Servis, *Nature (London)*, **227**, 1047 (1970).
(8) F. A. Sedor, D. G. Jacobson, and E. G. Sander, *Bioorg. Chem.*, **3**, 221 (1974).
(9) R. L. Blakley, "The Biochemistry of Folic Acid and Related Pteridines", Wiley, New York, N.Y., 1969.
(10) R. J. Langebuch, P. V. Danenberg, and C. Heidelberger, *Biochem. Biophys. Res. Commun.*, **48**, 1565 (1972).
(11) A. Albert, W. L. F. Armarego, and E. Spinner, *J. Chem. Soc.*, 2689 (1961).
(12) M. J. Cho and I. H. Pitman, *J. Am. Chem. Soc.*, **96**, 1843 (1974).
(13) E. G. Sander and W. P. Jencks, *J. Am. Chem. Soc.*, **90**, 6154 (1968).
(14) O. Manousek and P. Zuman, *Chem. Listy*, **49**, 668 (1955).
(15) I. H. Pitman and M. Ziser, *J. Pharm. Sci.*, **59**, 1295 (1970).
(16) R. F. Nelson in "Technique of Electroorganic Synthesis", N. L. Weinberg, Ed., Wiley, New York, N.Y., 1975.
(17) A. Albert and W. L. F. Armarego, *Adv. Heterocycl. Chem.*, 41 (1965).
(18) A similar criterion for reversibility and the number of electrons in the reaction was used in ref 20.
(19) B. J. Tabner and Y. R. Yaudle, *J. Chem. Soc. A*, 381 (1966).
(20) D. L. Smith and P. J. Elving, *J. Am. Chem. Soc.*, **84**, 2741 (1962).
(21) D. L. Smith and P. J. Elving, *Anal. Chem.*, **34**, 930 (1962).
(22) J. Volke, "Physical Methods in Heterocyclic Chemistry", Vol. 1, A. R. Katritzky, Ed., Academic Press, New York, N.Y., 1963, p 239.
(23) D. D. Perrin in "Dissociation Constants of Organic Bases in Aqueous Solution", Butterworths, London, 1965.
(24) H. Lund, *Acta Chem. Scand.*, **18**, 1984 (1964).
(25) Unpublished observation from our own laboratory.

Evaluation of Possible SN2 Transition-State Models for Reaction of *n*-Butyl Chloride Using Chlorine Kinetic Isotope Effects[1]

Robert L. Julian and James W. Taylor*

Contribution from the Department of Chemistry, University of Wisconsin, Madison, Wisconsin 53706.

Received May 19, 1975

Abstract: A series of possible transition-state models for the reaction of *n*-butyl chloride with thiophenoxide anion in methanol is evaluated using chlorine kinetic isotope effects (KIE). Vibrational analysis of a skeletal ground-state model, assuming a point propyl group, reproduces the experimentally measured normal modes of both isotopically substituted molecules to an average error of ±0.030%. The central transition-state model results in KIE values of 1.00898 and 1.00791 at 20 and 60 °C, respectively, compared to observed values of 1.0089_8 and 1.0079_2. The correlation of KIE values with transition-state geometry shows that the C–Cl and C–H bond lengths correlate well with the difference in KIE values at 20 and 60°. The C–C bond length correlates to the temperature-dependent factor and the approach to planarity of the groups attached to the central carbon correlates with the temperature-independent factor. The most consistent model results in C–Cl = 1.186, C–C = 1.533, C–H = 1.110 Å, ∠Cl–C–C = 93.1, ∠Cl–C–H = 92.9, ∠C–C–H = 119.5, and ∠H–C–H = 116.2°. Calculated α-deuterium isotope effects for this model are in good agreement with those observed for a similar reaction.

Introduction

Experimental measurements of kinetic isotope effects (KIE) have shown great utility as a probe for reaction mechanisms.[2-4] The leaving group heavy-atom values have also been found to be very sensitive to the transition state structure[5-8] and are also useful in evaluating conflicting mechanistic explanations.[9] However, because theoretical KIE calculations require knowledge of all ground-state and transition-state frequencies as well as their isotopic shifts,[10] few rigorous model calculations

have been made on physical systems which are observed experimentally and most transition-state information has been made by inference.[11-13] In addition to the measured values, the temperature dependence of KIE also holds some promise of providing additional information. Wolfsberg and Stern[14] have studied the KIE temperature dependence of methyl halide-type systems and Stern et al.[15,16] have studied variations in temperature dependences of equilibrium isotope effects of almost 700 systems. These equilibrium calculations, however, do not directly account for reaction transition states and, consequently, provide somewhat less information about them. Complete model studies of the KIE temperature dependence and conclusions about the transition state of intramolecular decarboxylation reactions have been made by Yankwich and co-workers.[17,18] Recently, in this laboratory we have used calculated leaving group KIE in a rigorous model study of the transition state of the methanol solvolysis of *tert*-butyl chloride.[19] In this study of a classic SN1 reaction, dependences of various geometric parameters of the transition state on the calculated KIE were evaluated. Large imaginary decomposition frequencies were *not* required to match experimental data and various predictions with regard to systems of lower symmetry were made.

It is the purpose of this paper to extend these model calculations in order to evaluate the transition state for a SN2 reaction using the reaction of *n*-butyl chloride with thiophenol anion in methanol and to compare the theoretical KIE calculations of various transition-state models with experimental data. This system was chosen as a representative of a class of SN2 reactions. It is uncomplicated by elimination reactions; it appears not to be complicated by ion-pair formation; and the C_s symmetry of *n*-butyl chloride is also much lower than the C_{3v} symmetry of *tert*-butyl chloride. These features also allow testing of some of our previous predictions.[19b] The temperature dependence of this reaction has been experimentally investigated in an earlier study,[11] and the data permit an evaluation of the transition-state structure in terms of various geometric parameters as well as the calculated KIE temperature dependence.

Experimental Section

Infrared Spectroscopy. Chemicals. Normal abundance *n*-butyl chloride was purchased as a liquid from Aldrich Chemical Co. The sample was degassed on the vacuum line by several freeze–thaw cycles using liquid nitrogen.

Apparatus. All spectra were taken on a DIGILAB FTS-20 Fourier transform infrared spectrophotometer. This instrument was determined to be accurate to within ±0.03 cm^{-1} by comparison with lines of polystyrene (1181.39, 1154.34, and 906.71 cm^{-1}) and water (456.87, 397.34, and 369.36 cm^{-1}). The highest resolution mode was checked by comparing measured lines of nitrous oxide with those given by Rao[20] and peaks with a separation of 0.15 cm^{-1} could be distinguished. All spectra were taken at this resolution with the entire optical system under constant nitrogen purge. Spectra were signal averaged, on the order of 2500 scans, and averaged background scans were subtracted to yield the final spectra. At this high resolution, many bands were resolved into their rotational fine structure. Peaks were measured at their observed Q branch maxima (or lack thereof). The reproducibility of the FTS-20 was found to be exceptional and within the earlier quoted ±0.03 cm^{-1} limit. The isotopic shifts could be determined directly from spectra of the normal abundance compound with an estimated uncertainty of ±0.1 cm^{-1} for most bands. In the measurement of the C–C–Cl bending vibration, however, a significantly larger uncertainty resulted due to water interference. Therefore, this mode was also measured with a SPEX RAMALOG laser Raman spectrophotometer using the 6471 Å line of a krypton laser as the source of excitation. The resulting uncertainty of this measurement was ±0.2 cm^{-1}.

Calculations. All computational work was done on a Univac 1110 digital computer with 32K of fast memory and 262K of low speed unitized memory.

The program used for vibrational analysis and kinetic isotope effect calculations is divided into three major subroutines. The first of these (VIB1) accepts basic geometric input data and internal coordinate data and generates the moments of inertia, Wilson's G matrix and its associated eigenvalues, and the Q matrix. The second subroutine (VIB2) accepts observed frequencies and a set of trial force constants and, using this data along with output data of VIB1, calculates frequencies, iterates the force constants if necessary, and calls the subroutine for calculation of kinetic isotope effects.

Subroutine KIE, the third major subroutine, which is called by VIB2, performs all kinetic isotope effect and associated calculations. This routine has been described previously[21] as have the algorithms used in computerized normal coordinate analysis. All the calculations assume simple harmonic oscillators and no correction for anharmonicity is made.

Results

Vibrational Assignments for the Ground State. A complete vibrational analysis of *n*-butyl chloride would involve 36 normal modes. A technique similar to the cut-off procedure of Wolfsberg and Stern[14] may be employed, where all vibrations associated with modes more than two bond lengths away from chlorine are built into the model by considering that portion of the molecule (an *n*-propyl group in the *n*-butyl chloride case) as a single atom. This results in a skeletal five-atom model requiring only nine normal modes for consideration.

Assigning a single internal coordinate description to a measured band is, at best, approximate, as shown by similar theoretical calculations.[19a] For solid-phase *n*-butyl chloride, Snyder and Schachtschneider[22] have calculated the distribution of potential energy amongst the various modes for each band. For bands in the 1440–850-cm^{-1} region, reasonable contributions by three or four modes per band are seen. The problem of choosing the nine appropriate measured bands for iterative calculations then, is one of choosing those bands in which the desired modes of interest are the predominant contributors. Using the potential energy distributions of Snyder and Schachtschneider, along with assignments in similar molecules[23] and trends in characteristic frequencies,[24] the nine ground-state normal modes required for KIE calculations were determined. These frequencies, *approximate* descriptions, and isotopic shifts are listed in Table I. The splittings are listed as positive when the heavier isotope peak appears at lower frequency. The use of the FTS-20 at 0.15-cm^{-1} resolution permitted most isotopic shifts to be determined from the normal abundance spectra. A brief discussion of each mode, along with other possible contributions, follows.

C–H Stretch (ν_1 and ν_7). Bands involving C–H stretching are expected not to mix with other modes as predicted by the high-frequency separation approximation.[25] For the entire molecule, six bands are expected in the 3000-cm^{-1} region due to methyl and methylene symmetric and asymmetric C–H stretches (four bands) plus two other bands due to symmetric and asymmetric stretch of the methylene associated with the chlorine. At appropriate pressures all six bands were observed and these latter two bands were extracted. No isotopic shift was expected or observed at the instrument resolution.

CH_2 Wag (ν_2). This bending mode usually contributes to bands in the 1400–1100-cm^{-1} region according to Snyder and Schachtschneider,[22] but the major contribution from methylene associated with Cl is at ca. 1458 cm^{-1}. The observed band at 1453.5 cm^{-1} was chosen for calculations because a definite isotopic shift was observed. There may be significant mixing by the methylene scissoring mode with this wagging mode.

CH_2 Scissor (ν_3). This mode is apparently not isolated in any band. However, its contributions appear to be about equal in the 1453.5 and 1318.2-cm^{-1} bands. The CH_2 wagging mode appears to be the major constituent for the 1453.5-cm^{-1} band and, therefore, the 1318.2-cm^{-1} band was assigned to the

Table I. Observed and Calculated Frequencies and Isotopic Shifts of *n*-Butyl Chloride Ground State

Approximate description	Measured		Calculated		
	Frequency, cm^{-1} [a]	Isotopic shift, cm^{-1} [a]	Frequency, cm^{-1}	% error	Isotopic shift, cm^{-1}
ν_1 C–H sym. stretch	2965.30		2964.46	0.028	0.01
ν_2 CH_2 wag	1453.50	0.30	1453.65	0.010	0.41
ν_3 CH_2 scissors	1318.20		1318.11	0.007	0.02
ν_4 C–C stretch	1021.80[b]	0.40[b]	1021.86	0.006	0.46
ν_5 C–Cl stretch	749.90[b]	4.90	749.70	0.027	4.50
ν_6 C–C–Cl bend	333.00[b,c]	1.40[b]	333.45	0.135	1.96
ν_7 C–H asym. stretch	2998.80		2999.45	0.022	0.00
ν_8 CH_2 twist	1243.80	0.50	1243.54	0.021	0.25
ν_9 CH_2 rock	876.30	0.30	876.40	0.011	0.22

[a] Uncertainties estimated from peak shape are ±0.10 cm^{-1} except where noted. [b] Uncertainty, ±0.20 cm^{-1}. [c] Measured by laser Raman.

scissoring mode for calculations. No isotopic shift was observed. Other mixing may come from normal (i.e., nonchlorine associated) CH_2 wagging and also normal CH_2 scissoring modes.

C–C Stretch (ν_4). Snyder and Schachtschneider's calculations[22] show this mode to be the major contribution to two bands, and solely to the band at 1016 cm^{-1}. The measured band at 1021.8 cm^{-1} was assigned to ν_4 because it has an isotopic shift of 0.4 cm^{-1}. Bands at slightly higher frequency are complicated by the methylene wagging motion, whereas the 1021.8-cm^{-1} band is not.

C–Cl Stretch (ν_5). This mode generally occurs in the 700–750-cm^{-1} region for normal chlorinated hydrocarbons. The measured value of 749.9 cm^{-1} is for the trans conformation, i.e., chlorine coplanar with the carbon chain. At room temperature ca. 70% of *n*-butyl chloride molecules are in this conformation.[26] The isotopic splitting of 4.9 cm^{-1} is considerably larger than the 3.5 cm^{-1} estimated earlier.[19a] The gauche conformational mode was measured at 668.1 cm^{-1}, which also showed a 4.9-cm^{-1} splitting.

C–C–Cl Bend (ν_6). This mode occurs in the far infrared region and is the most uncertain of the bands measured with the FTS-20 due to interferences from water bands. To improve this measurement, the band was examined with the laser Raman system, as the Raman spectrum of water is quite weak. The position and isotopic shift are much more certain with this measurement than with the FTS-20. The band at 333.0 cm^{-1} was chosen even though the C–C–C bending mode contributes to a greater extent. This latter mode is more closely associated with the band at 474.5 cm^{-1} which is *not* shifted, while the 333.0-cm^{-1} band has a definite shift.

CH_2 Twist (ν_8). This mode also occurs in the 1400–1100-cm^{-1} region. The twisting of the methylene group associated with chlorine appears at 1251 cm^{-1} for ethyl chloride.[23] The band at 1243.8 cm^{-1} was chosen for *n*-butyl chloride and is split by 0.5 cm^{-1}. There may also be significant mixing by the normal methylene rock, methyl rock, and normal methylene twisting modes.

CH_2 Rock (ν_9). This mode contributes to many bands and, like ν_3, is not the major contribution to any band. Its contribution appears highest in the measured band at 876.3 cm^{-1}, which is shifted by 0.3 cm^{-1}. This is at a higher frequency compared to normal methylene rocking modes usually found around 800 cm^{-1}, but is considered reasonable as this mode appears at 1036 cm^{-1} in ethyl chloride.[23] This band may also have slight mixing by normal CH_2 rock and twist modes.

The torsional modes involving the chlorine atom need not be considered here, as they have little meaning for the five-atom skeletal model. An estimation of possible contributions by other modes to the assigned bands used may be obtained from the eigenvectors resulting from ground-state analysis.

Ground-State Computational Model for *n*-Butyl Chloride. Normal coordinate analysis was performed on a ground-state model for *n*-butyl chloride in order to determine a force field which would theoretically reproduce the measured ground-state frequencies and their isotopic shifts. This force field could then be changed appropriately for a given transition-state model and the transition-state frequencies calculated for kinetic isotope effect calculations. The programs used were adopted from previous work[21] and modified for this application. The FG matrix methods of Wilson were employed.[25] The ground-state model used was an isotopically invariant methyl chloride skeleton with a point propyl group of mass 8.357 amu. This mass was calculated using *n*-propyl chloride shift data,[19a] assuming the propyl group to be a point mass. There are seven different types of internal coordinates for this molecule (C_s symmetry) for a total of ten, giving rise to the model shown in Figure 1. The coordinate values used in the calculation of the ground-state model are also presented in this figure. Data for r, R, R, γ, and Δ were taken from the electron diffraction data of Ukaji and Bonham.[27] The values of α and β were determined by considerations which resulted in a spherically complete model, i.e., all six angles are not completely independent. Once five angles are specified, the sixth is already determined. Preliminary calculations showed that slight changes in the geometric parameters or point propyl mass would not significantly affect this model. For example, the reported uncertainty of the C–Cl bond length is 0.004 Å.[27] A change in R of this magnitude altered the calculated frequency of only one vibration (ν_2) by barely 0.1%. Calculations of angular changes showed that variation of angle Δ affected the most significant changes in calculated values. A change of 1.0° was required to alter the vibrational values of up to 0.5%. In addition, it was determined that no variation of any geometric parameter of up to 1.0% caused a change in any calculated isotopic splitting of more than 0.01 cm^{-1}. This splitting is even more important in calculations of kinetic isotope effects than the exact vibrational frequency.

With nine normal modes of the skeletal model and ten internal coordinates, one redundancy condition exists. Group theoretical calculations of the C_s point group show that six of the modes exhibit A′ symmetry, i.e., totally symmetric modes, and three exhibit A″ symmetry, i.e., asymmetric with respect to the plane of reflection. They also show the redundant condition to be of A′ symmetry. It was initially decided to attempt the use of both general valence and symmetry force constants so a more generalized approach would be applicable to molecules of different symmetry. For *n*-butyl chloride, however, there is little symmetry. In this case the use of symmetry force constants is not beneficial and only the general valence force

Table II. General Valence Force Field[a,b] for *n*-Butyl Chloride Ground-State Model

f(r-r) = 4.855	f(r-r′) = 0.059	f(r-*R*) = 0.000	f(β-*R*) = −0.230	f(α-Δ) = 0.000
f(β-β) = 1.172	f(r-β) = 0.000	f(r-R) = 0.000	f(β-R) = 0.496	f(α-*R*) = −0.024
f(γ-γ) = 0.609	f(r-β′) = 0.000	f(β-β′) = 0.340	f(γ-γ′) = −0.034	f(α-R) = −0.116
f(α-α) = 0.373	f(r-γ) = 0.000	f(β-γ) = 0.105	f(γ-α) = −0.030	f(Δ-*R*) = 0.139
f(Δ-Δ) = 0.562	f(r-γ′) = 0.000	f(β-γ′) = 0.083	f(γ-Δ) = −0.004	f(Δ-R) = −0.054
f(*R*-*R*) = 3.579	f(r-α) = 0.000	f(β-α) = 0.099	f(γ-*R*) = 0.000	f(*R*-R) = 0.758
f(R-R) = 3.479	f(r-Δ) = 0.000	f(β-Δ) = 0.009	f(γ-R) = 0.000	

[a] Refer to Figure 1 for notation. [b] All values in mdyn/Å.

Table III. Normalized Eigenvectors[a] of *n*-Butyl Chloride Ground State

	r_1	r_2	β_1	β_2	γ_1	γ_2	α	Δ	*R*	R
ν_1	1.000	1.000					−0.162			
ν_2			1.000	1.000	−0.663	−0.633	−0.680			
ν_3			−0.315	−0.315	−0.430	−0.430	1.000		0.169	
ν_4			0.115	0.115	0.417	0.417	−0.777	−0.303	1.000	
ν_5			−0.321	−0.321	0.196	0.196	0.890	−0.609	−0.308	1.000
ν_6			−0.119	−0.119	−0.249	−0.249	−0.293	1.000		0.189
ν_7	1.000	−1.000	−0.100	0.100	−0.109	0.109				
ν_8			−1.000	1.000	0.884	−0.884				
ν_9			−0.671	0.671	−1.000	1.000				

[a] Refer to Figure 1 for notation.

fields are used throughout the remaining portions of this work.

Only the more predominant trans configuration is considered in these calculations. The gauche form, being of C_1 symmetry, is a slightly different problem. The neglect of this conformation may slightly affect the calculated KIE values, but the temperature dependence should be the same for both cases.

Ground-State Force Field of *n*-Butyl Chloride. A general valence force field was prepared by explicit use of transferability of force constants from similar molecules. Data from *n*-butyl chloride,[22] ethyl chloride,[28] secondary chlorides,[29] *tert*-butyl chloride, and methyl chloride,[21] as well as from other sources[30] were considered and a final set was proposed. This field was used directly in the internal force field and was also transformed to a symmetry force field. Iterative improvement was made using all nine skeletal frequencies (ν_6 being weighted less initially) as well as the six isotopic shift frequencies. The practice was to fix all but four or five constants of interest and let the program iterate these three or four times. The effect of changes of each force constant could be determined by the resulting Jacobian matrix. Predictions were made between runs as to which force constants should be varied in the next run. Iteration proceeded in this manner and the force field was adjusted until the following criteria were met: (1) all calculated frequencies of *both* isotopic species were within 1% of the observed values; (2) all eigenvectors showed that the largest contribution to a given normal mode was that due to the internal coordinate used to describe it; e.g., r (C–H bond) is the largest contribution to ν_1 (C–H stretch); (3) the resulting force constants were not substantially different from those reported for similar molecules. With all of these criteria met, it was reasonably certain that a physically meaningful force field had been attained. From this point the field was further adjusted until the best possible set of frequencies resulted. The final general valence force field is presented in Table II. A comparison of the calculated frequencies and isotopic shifts with those observed is given in Table I. The agreement between theoretical and experimental frequencies is very good, with the worst-case error of only ±0.14%. The average error is 0.030%. The calculated isotope shifts also agree quite well with measured data; the most outstanding deviation being the rather large shift for ν_6. Table III gives the eigenvectors (normalized by dividing each value by the largest value) which resulted from these calculations. They show the relative amounts of mixing of the modes for each vibration. It is of interest to examine these modes with regard to the predictions made earlier when assigning the bands.

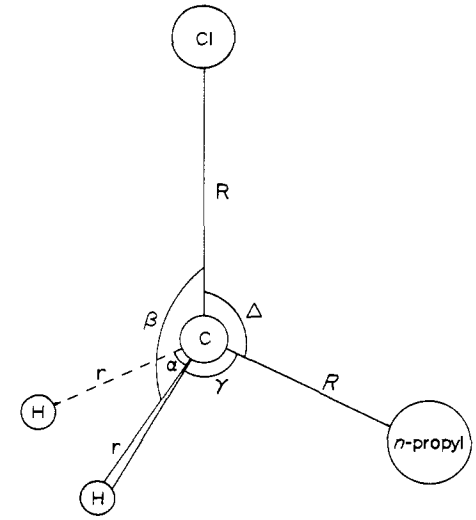

Figure 1. Ground-state model of *n*-butyl chloride. Values of bond lengths (Å) are: R = 1.780, *R* = 1.533, and r = 1.110. Values of angles (deg) are: α = 108.2, β = 109.2, γ = 109.9 and Δ = 110.8.

The high frequency separation approximation appears valid here as ν_1 and ν_7 are relatively free of mixing and, as predicted, are almost entirely C–H stretch. It is also apparent that the various angle bending modes are quite complicated, as expected. As predicted, the CH_2 wagging mode (ν_2) has a large contribution by the α coordinate associated with CH_2 scissoring. It also has mixing from the γ coordinate. The same trend occurs between the twist and rock modes (ν_8 and ν_9), which show strong intermixing. The predicted mixing of the β coordinate with the methylene scissoring mode (ν_3) is clearly shown, plus an unexpected mixing to an even greater extent by the γ coordinate. The C–C and C–Cl stretching modes (ν_4 and ν_5) have large contributions by other coordinates, espe-

Table IV. Transition-State Model 1 for *n*-Butyl Chloride[a]

r = 1.110 Å	α = 108.2°
R = 1.869 Å	β = 90.0°
R = 1.533 Å	γ = 125.9°
	Δ = 90.0°

[a] Refer to Figure 1 for notation.

cially the α coordinate. Finally, the C-C-Cl bending mode has several other weak contributions.

***n*-Butyl Chloride Initial Transition-State Model.** In order to develop a complete transition-state model for the reaction of interest, the essential problem is that both the transition-state geometry and force field are intimately coupled. A basic model is needed, calculations from which reproduce the experimental KIE data to some degree of accuracy. From this basic model, the effects of changes in various model parameters can be examined. With this in mind, a reasonable geometric model was proposed and the ground-state force field adjusted, subject to a number of criteria discussed below, to reproduce the experimental data. The necessary adjustment of the force field gives the dependences of the system on various force constants. From this total model then, effects due to variation of geometric parameters could be studied.

All of the principal assumptions implicit in the ground-state model are incorporated into all the transition-state models. Specifically, the vibrations of the *n*-propyl group itself are built into that group as a unit, and only the skeletal modes are considered. Relative thermodynamic properties are calculated from *ratios* of partition functions. Therefore, frequencies considered to be similar may be ignored and the use of a skeletal model is an adequate description of the system.

The problem in choosing the basic model from which to make variations begins with the choice of a reasonable geometry. As the reaction progresses one must view the C-Cl bond as increasing in length until it no longer may be considered as a vibration. As this proceeds, the two hydrogens and the *n*-propyl group may be described as approaching an inversion process, while the nucleophile approaches the side opposite the leaving chlorine atom. The true transition-state geometry may be envisioned as some intermediate composite of all three processes. The maximum C-Cl distance that will be considered will be that distance beyond which small changes cease to have any appreciable effect on the KIE results. Preliminary calculations show this to be about 4.48 Å (the ground-state value is 1.78 Å). In a study of a similar reaction, the SN2 solvolysis of benzyl bromide, Bron[31] used a trigonal bipyramidal transition-state geometry. From linear free-energy considerations, e.g., the Hammond postulate,[32] we would also predict the transition state of *n*-butyl chloride to be reactant-like. On the basis of these considerations, a geometry was chosen such that the two hydrogens, the central carbon, and the point propyl group all lie in the same plane (the *xy* plane) with the C-Cl bond perpendicular to this plane. Consistent with the results of Bürgi,[33] which show that the lengths of equatorial bonds remain essentially unchanged during SN2-like inversion, the C-H and C-propyl bond lengths for this geometry were retained at ground-state values as was the value of angle α for simplicity in geometric considerations. The increased length in the C-Cl bond is somewhat arbitrary. Other workers have done calculations in which this bond length has been increased by no more than 25%, and usually only a few percent.[7,13] A value of 1.869 Å, an increase of 5% over the ground-state value, was chosen. This basic geometry, model 1, is presented in Table IV.

This model poses an interesting problem if one is to consider a form of concerted transition state. The transition-state models generally proposed approximate the line of direct approach of nucleophile to carbon as being along the negative *z* axis (considering the C-Cl bond as being along the positive *z* axis). If one begins from the ground state of the reactants, there are, however, no internal coordinates to describe the nucleophile position. No new coordinates can be introduced, if one retains the same general force field as in the reactant ground state. Assignment of the angle of approach of the nucleophile then, in this first approximation, must remain undefined.

Transition-State Force Field for *n*-Butyl Chloride. With the formation of transition-state model 1, a reasonable transition-state force field is required in order to study various other geometric models. The choice of force constants is not obvious and a set cannot be transferred from similar molecules, as was done in the ground-state case. It is not possible to employ iteration because the transition-state frequencies cannot be measured. Experimental values which do permit an evaluation of the models, however, are the measured kinetic isotope effect values. A reasonable force field should reproduce these values and their associated temperature dependence, to within experimental error. Therefore, the following criteria were used to convert the ground-state force field to the desired transition-state field: (1) The calculated KIE value at 20 °C should match the measured value of 1.0089_8[35] to within the experimental error of $\pm 0.0001_5$. (2) The calculated KIE values should reproduce the measured temperature dependence. The KIE values vary almost linearly over the range of 20–60 °C. Therefore, the difference in KIE values at 20 and 60 °C can reflect this temperature dependence. This is general, however, and is not the temperature-dependent factor (TDF). The observed experimental value is 10.6×10^{-4}. (3) The resulting decomposition frequency, ν_L, should be zero or a small imaginary value to avoid the complications cited by Williams and Taylor[19b] concerning the very large tunneling coefficients. (4) The isotopic shift of ν_L should be quite small, as theory predicts little isotopic dependence in the transition state. (5) The resulting eigenvectors should show the same basic dependences as in the ground state. The amount of mixing, however, may be quite different from that of the ground state. If all of these conditions are met, one can be reasonably confident in having a force field of physical significance for examining geometric dependences. The experimental KIE data are for the solution-phase reaction, but solution effects can be assumed to cancel in the ratios to a first approximation,[11] and these data may be used with gas-phase vibrational assignments.

Initially, only the diagonal force constants were varied and all off-diagonal elements held at their ground-state values. Coupled to the increase in the C-Cl bond length, R, there is a decrease in the effective potential energy of the C-Cl stretching mode. This, along with the decrease in bonding involved, resulted in the expected large decrease in f(R-R). An increase in effective potential energy is associated with the decrease in β and Δ angles and requires the increase of $f(\beta\text{-}\beta)$ and $f(\Delta\text{-}\Delta)$. This same reasoning would predict a decrease in $f(\gamma\text{-}\gamma)$, as γ angles were increased. However, this decrease was not diagnostic. This was attributed to the fact that the changes in γ were not as large as the changes in β or Δ, or more likely, that γ angles do not increase as much as given in model 1, and are accompanied instead by an increase in α.

The diagonal-constant dependences could then be used to predict the diagnostic changes in off-diagonal (i.e., interaction) force constants. If a diagonal force constant increases, this implies that its associated mode is more self-interacting and might be expected to interact to a lesser extent with other modes. All off-diagonal elements associated with an increasing diagonal element might be expected to decrease, and vice versa. Thus, consistent with this idea, increases in $f(\gamma\text{-R})$, $f(\alpha\text{-R})$, and $f(R\text{-R})$ along with decreases in $f(\beta\text{-}\Delta)$ and $f(\Delta\text{-}R)$ proved useful in matching the experimental KIE values. All other constants remained at ground-state values because no changes

Table V. Transition-State Force Field 1[a,b] for *n*-Butyl Chloride

f(r-r) = 4.855/100%[c]	f(r-α) = 0.000/0.000	f(γ-γ') = −0.034/0.000
f(β-β) = 1.353/115%	f(r-Δ) = 0.000/0.000	f(γ-α) = −0.030/0.000
f(γ-γ) = 0.609/100%	f(r-*R*) = 0.000/0.000	f(γ-Δ) = −0.004/0.000
f(α-α) = 0.373/100%	f(r-R) = 0.000/0.000	f(γ-*R*) = 0.000/0.000
f(Δ-Δ) = 0.649/116%	f(β-β') = 0.340/0.000	f(γ-R) = 0.261/0.261
f(*R*-*R*) = 3.579/100%	f(β-γ) = 0.105/0.000	f(α-Δ) = 0.000/0.000
f(R-R) = 0.974/28%	f(β-γ') = 0.083/0.000	f(α-*R*) = −0.024/0.000
f(r-r') = 0.059/0.000[d]	f(β-α) = 0.099/0.000	f(α-R) = −0.005/0.111
f(r-β) = 0.000/0.000	f(β-Δ) = −0.283/−0.292	f(Δ-*R*) = −0.625/−0.764
f(r-β') = 0.000/0.000	f(β-*R*) = −0.230/0.000	f(Δ-R) = −0.054/0.000
f(r-γ) = 0.000/0.000	f(β-R) = 0.496/0.000	f(*R*-R) = 0.927/0.169
f(r-γ') = 0.000/0.000		

[a] Refer to Figure 1 for notation. [b] All values in mdyn/Å. [c] Percent of ground-state value given for diagonal values. [d] Difference from ground-state value given for off-diagonal values.

Table VI. Calculated Transition-State Frequencies and Isotopic Shifts for Reaction of *n*-Butyl Chloride Using Model 1 and Force Field 1.

	Transition state		Ground state		Transition state − ground state, cm^{-1}
	n-Bu^{35}Cl, cm^{-1}	Isotopic shift, cm^{-1}	*n*-Bu^{35}Cl, cm^{-1}	Isotopic shift, cm^{-1}	
ν_1	2968.49	0.00	2964.46	0.01	4.03
ν_2	1610.81	0.57	1453.65	0.41	157.16
ν_3	1494.79	0.11	1318.11	0.02	176.68
ν_4	1148.00	0.53	1021.86	0.46	126.14
ν_L	24.22[a]	0.08	749.70	4.50	−773.92
ν_6	249.12	2.11	333.45	1.96	−84.33
ν_7	3001.45	0.00	2999.45	0.00	2.00
ν_8	1224.38	0.33	1243.54	0.25	−19.16
ν_9	1070.77	0.09	876.40	0.22	194.37

[a] This value of ν_L is imaginary.

Table VII. Transition-State Models Generated Around Model 1[a]

	Bond lengths, Å			Angles, deg				
Model	R	*R*	r	Δ	β	γ	α	MMI
1	1.869	1.533	1.110	90.0	90.0	125.9	108.2	1.0002
2	1.869	1.533	1.110	*110.8*	*109.2*	*109.9*	108.2	0.9998
3	1.869	1.533	1.110	*105.6*	*104.4*	*113.2*	108.2	0.9999
4	1.869	1.533	1.110	*100.4*	*99.6*	*117.2*	108.2	1.0000
5	1.869	1.533	1.110	*95.2*	*94.8*	*121.2*	108.2	1.0001
6	1.869	1.533	1.110	*94.2*	*93.8*	*122.7*	108.2	1.0001
7	1.869	1.533	1.110	*93.1*	*92.9*	*123.5*	108.2	1.0001
8	1.869	1.533	1.110	*92.1*	*91.9*	*124.3*	108.2	1.0002
9	1.869	1.533	1.110	*91.0*	*91.0*	*125.1*	108.2	1.0002
10	1.869	1.533	1.110	*89.0*	*89.0*	*125.1*	108.2	1.0002
11	1.869	1.533	1.110	*84.8*	*85.2*	*121.2*	108.2	1.0003

[a] Italicized values represent changes from model 1.

were observed in the associated diagonal elements, or opposing changes in the two diagonal elements associated with a given interaction element, or because the relative magnitudes of change were insufficient to affect the off-diagonal elements.

The field was adjusted in accordance with these predictions until all the criteria were met. The final set of force constants, force field 1, is presented in Table V. The relative percentages of ground-state values are given for diagonal elements, while differences are given for off-diagonal constants. The calculated transition-state frequencies and their isotopic shifts for model 1 and force field 1 are presented in Table VI. The suffixes R and I on ν_L values throughout the rest of this work indicate real and imaginary frequencies, respectively. All other frequencies are real. The ground-state values are also given for reference, and the difference in magnitudes of vibrations between the transition state and the ground state is given in the final column of Table VI.

Finally, a series of models (2–11) was developed to show the effects of a smooth inversion process from the ground-state angles to an inversion ca. 25% beyond the planar configuration of model 1. The internal coordinates of all of these models are presented in Table VII. This table also lists the MMI (mass times moment of inertia) term, as this is fixed by the geometry of a given model. Results of this smooth inversion study indicated that the transition state might be better described by a model similar to model 7, which corresponds to about 85% of the inversion from ground-state angles to the planar model 1. For the new central configuration, model 12 was created and several other models (13–20) were generated around this. These later models, along with model 7 for comparison, are shown in Table VIII.

In the models previously considered, no coordinates were explicitly included for the nucleophile. These can be included, however, by making some additional assumptions as follows:

Table VIII. Transition-State Models Generated Around Model 12[a]

Model	Bond lengths, Å			Angles, deg				MMI
	R	*R*	r	Δ	β	γ	α	
7	1.869	1.533	1.110	93.1	92.9	123.5	108.2	1.0001
12	1.816	1.533	1.110	93.1	92.9	119.5	116.2	1.0002
13	1.816	1.533	1.110	*100.4*	*99.6*	*115.6*	*112.9*	1.0001
14	1.816	1.533	1.110	*95.2*	*94.8*	*118.4*	*115.3*	1.0002
15	1.816	1.533	1.110	*94.2*	*93.8*	*118.9*	*115.7*	1.0002
16	1.816	1.533	1.110	*92.1*	*91.9*	*120.1*	*116.7*	1.0003
17	1.816	1.533	1.110	*91.0*	*91.0*	*120.6*	*117.1*	1.0003
18	1.816	1.533	1.110	*90.0*	*90.0*	*121.2*	*117.6*	1.0003
19	1.816	1.533	1.110	*87.9*	*88.1*	*120.1*	*116.7*	1.0004
20	1.816	1.533	1.110	*84.8*	*85.2*	*118.4*	*115.3*	1.0004

[a] Italicized values represent changes from model 12.

(1) It appears to be somewhat uncertain as to whether or not the nucleophile should be included in the ground-state model as an entity at long distance from and not reacting with (i.e., all force constants zero) the *n*-butyl chloride.[36] It seems unrealistic to include it, as the program necessarily calculates the moment of inertia under the assumption that the entire molecule is rigid. In the absence of better methods, we have chosen to include the nucleophile only in the transition-state model. (2) For the transition state, four new internal coordinates and an additional 31 force constants may be introduced to include the nucleophile. It is necessary to estimate the S–C length and the three diagonal force constants $f(\Phi\text{-}\Phi)$, $f(\theta\text{-}\theta)$, and $f(\phi\text{-}\phi)$, where Φ is the stretching of the S–C bond, θ is the bending of ∠S–C–H, and φ is the bending of ∠S–C–C. We can use the relationship from Pauling:[37] $R^{\pm} = R - 0.300 \log (n)$, where *n* is the bond order and $R^{\pm}$ and R are the C–X bond lengths in the transition state and ground state, respectively. With model 12, the transition state C–Cl bond length is 1.816 Å compared to the ground-state value of 1.780 Å. In this case the value of *n* becomes 0.758. Using a typical value for the C–S bond length of 1.780 Å in the ground state and a value of $n = 0.242$ (assuming $n_{C\text{-}X} + n_{C\text{-}S} = 1$), we obtain a transition-state value of 1.965 Å for the C–S length. From the recent paper by Bron[31] we can obtain the relationships needed for the other diagonal force constants as follows: $f(\Phi\text{-}\Phi) = 5.72(n_{C\text{-}S}) = 1.384$ mdyn/Å; $f(\theta\text{-}\theta) = f(\phi\text{-}\phi) = 0.283(n_{C\text{-}S}) = 0.068$ mdyn/Å. The influence of these assumptions on the various force constants of transition-state force field 2, optimized for model 12 (discussed below), and the influence on the moment of inertia term is shown in Table IX.

Kinetic Isotope Effect Calculations. Given a transition-state force field and any given geometric transition-state model, the KIE, TIF, TDF, and Wigner tunnel coefficients can be calculated by subroutine KIE. A plot of the logarithm of the calculated KIE values against inverse temperature is linear over the temperature range of experimental interest (ca. 0–60 °C). The vast amount of data for each model can, therefore, be compressed and models contrasted by specifying a representative point and the slope of this line for each model. As a close approximation to this, the point will be represented by the KIE value at 20 °C (KIE-20), and the slope by the difference between values at 20 and 60 °C (20–60 difference). These are the same parameters that were used for adjustment of the transition-state force field. This latter difference will be referred to as the temperature dependence, but it should be noted that this is not the temperature-dependent factor (TDF). All data show this same linear behavior and only the KIE-20 and 20–60 difference values are reported for comparison. The experimentally observed KIE-20 value is $1.0089_8 \pm 0.0001_5$ and the 20–60 difference is $(10.6 \pm 0.2) \times 10^{-4}$.[35]

Table IX. Force Constant and MMI Terms with and without the Nucleophile in the Transition State

f(i-j)	Ground state	Transition state	
		Without N[a]	With N[b]
f(R-R)	3.479	0.974	1.010
f(β-R)	0.496	0.519	0.505
f(Φ-Φ)			1.384
f(θ-θ)			0.068
f(φ-φ)			0.068
f(θ-θ′)			−0.065
f(θ-φ)			−0.077
f(R-Φ)			0.007
MMI		1.0002	1.0032

[a] Using model 12 and force field 2. [b] Using model 12 and assumptions concerning bond lengths and bond orders as previously discussed. All force constants not specified maintain their force field 2 values.

The output of subroutine KIE contains both the Teller–Redlich temperature-dependent factor (VP·ZPE·EXC)[21] and the equivalent expression calculated using the rigorous partition function expression.[10] As seen also in similar studies[19b] we find these to be equivalent to within computer round-off error. This is to be expected, as a simple harmonic oscillator model was assumed throughout. The reported summaries, therefore, will contain only the Teller–Redlich TDF. The KIE data calculated for models 1–11 are presented in Table X. The effect of the tunnel coefficient for decomposition frequencies of this magnitude was found to be very small (0.00001 or less except for model 11, where the total value was 1.00003).

Evaluation of the data presented in Table X forces consideration of several questions about the choice of central geometric model and force field. The fact that $f(\gamma\text{-}\gamma)$ was not decreased (because of the increase in angle γ) is puzzling and the decrease in $f(\Delta\text{-}R)$ seems quite large. Also, the calculated frequencies of ν_2, ν_3, and ν_9 seem further from ground-state values than might have been expected for a SN2 (reactant-like) transition state. The KIE-20 data with regard to the smooth inversion process (models 2–11) show an interesting effect. Smooth inversion is taken as changes of all angles equal to the same percentage of the difference between their ground-state values and those of model 1. This means that all angles will attain their model 1 values at the same time. The models corresponding to 75% of this process between ground state and model 1 and beyond all show approximately the same temperature dependences. The KIE-20 values for these models (5–11) can therefore be compared. This correlation is parabolic in nature, showing a decrease in KIE with increasing inversion

Table X. Summary KIE Data for Models 1–11 Using Force Field 1, and Models 12–20 Using Force Field 2

Model	KIE-20	20–60 diff × 10^4	ν_{35L}[a]	ν_{35L}/ν_{37L}	ZPE[b]	EXC·ZPE[b]	VP	TDF[b]
1	1.00893	10.8	24.22I	1.0036	1.01013	1.00872	0.9965	1.00527
2	1.01554	10.3	239.39R	1.0103	1.00843	1.00533	0.9998	1.00516
3	1.01536	10.3	233.65R	1.0101	1.00856	1.00526	0.9999	1.00516
4	1.01040	10.5	197.44R	1.0052	1.00879	1.00520	1.0000	1.00519
5	1.00889	10.6	118.63R	1.0035	1.00920	1.00514	1.0001	1.00523
6	1.00884	10.6	100.45R	1.0035	1.00931	1.00513	1.0001	1.00524
7	1.00881	10.8	81.76R	1.0034	1.01015	1.00868	0.9966	1.00530
8	1.00883	10.8	60.98R	1.0035	1.01013	1.00867	0.9966	1.00528
9	1.00886	10.7	36.58R	1.0036	1.01013	1.00868	0.9966	1.00527
10	1.00901	10.8	44.84I	1.0037	1.01014	1.00878	0.9965	1.00527
11	1.00950	10.8	59.10I	1.0042	1.01028	1.00917	0.9962	1.00528
12	1.00898	10.7	36.21I	1.0036	1.01009	1.00873	0.9965	1.00525
13	1.00991	10.5	168.82R	1.0047	1.00888	1.00508	1.0001	1.00518
14	1.00903	10.7	73.32R	1.0038	1.01017	1.00884	0.9965	1.00527
15	1.00899	10.7	42.00R	1.0037	1.01012	1.00877	0.9965	1.00526
16	1.00899	10.7	63.36I	1.0037	1.01008	1.00873	0.9965	1.00524
17	1.00903	10.7	78.63I	1.0038	1.01007	1.00873	0.9965	1.00523
18	1.00908	10.7	89.28I	1.0038	1.01008	1.00876	0.9965	1.00523
19	1.00922	10.6	101.18I	1.0040	1.01009	1.00885	0.9964	1.00522
20	1.00954	10.7	104.79I	1.0043	1.01017	1.00908	0.9962	1.00522

[a] R and I suffixes refer to real and imaginary frequencies, respectively. [b] Values at 20 °C.

Table XI. Changes in Force Field 1 to Form Force Field 2[a,b]

Force field 1	Force field 2	Ground state field
$f(\beta\text{-}\beta) = 1.353$	1.315	1.172
$f(\gamma\text{-}\gamma) = 0.609$	0.557	0.609
$f(\alpha\text{-}\alpha) = 0.373$	0.339	0.373
$f(\Delta\text{-}\Delta) = 0.649$	0.631	0.562
$f(\beta\text{-}\Delta) = -0.283$	−0.275	0.009
$f(\beta\text{-R}) = 0.496$	0.519	0.496
$f(\Delta\text{-}R) = -0.625$	−0.586	0.139
$f(\Delta\text{-R}) = -0.054$	−0.037	−0.054

[a] Values in mdyn/Å. [b] Refer to Figure 1 for notation.

until about 85% of the way to the planar configuration of model 1. At this point the values hit a definite minimum and begin to increase as the inversion proceeds toward the planar configuration. The temperature-dependent factor is essentially constant for models 5–11. Thus, the minimum reflects a minimum in the ν_{35L}/ν_{37L}, the temperature-independent factor (TIF) of Yankwich and co-workers.[17]

Because these results indicated a problem with the initial models, a new central configuration (model 12) was generated which, along with a force field optimized to this new geometry, would reproduce the experimental KIE data. Model 12 corresponds to inversion about 85% of the way to model 1, i.e., slightly nonplanar and more reactant-like. The geometric considerations for this new model required an increase of the C–Cl bond by only 2% over the ground-state value (in contrast to 5% increase for model 1) and an increase in angle α. A comparison of the changes in force field 1 required to produce force field 2, optimized for this model by the procedure discussed earlier, is presented in Table XI. It is of interest that both $f(\alpha\text{-}\alpha)$ and $f(\gamma\text{-}\gamma)$ had to be decreased from ground-state value, as predicted earlier, as both angles α and γ have increased. The decrease in $f(\Delta\text{-}R)$ is not as severe as in field 1 and $f(\beta\text{-R})$ and $f(\Delta\text{-R})$ have now been *increased* over ground-state values, which would have been predicted because $f(\text{R-R})$ decreased by such a large amount compared to the increase in $f(\beta\text{-}\beta)$ and $f(\Delta\text{-}\Delta)$. The calculated frequencies for this model are also somewhat closer to reactant vibrations (ν_2 = 1558.11, ν_3 = 1442.29, ν_9 = 1042.69 cm^{-1}). In order to test the inversion process around this new central model, models 13–20 (Table VIII) were generated. The KIE results for these new models are also presented in Table X. Again these models showed the same temperature dependences, and the KIE-20 values may be compared. The same minimum in KIE-20 occurs, this time at the new central model value. This correlation implicitly shows the dependences of the TIF on the degree of planarity of the transition-state model, as the TDF changes only slightly from model to model. The TIF values also show a minimum value at model 12. The normalized eigenvectors for model 12 and force field 2 are given in Table XII. The calculated KIE values for model 12 and force field 2 are compared with experimental values in Table XIII. The KIE data for the transition state, which includes the nucleophile, is also listed as part of Table XIII.

Discussion

Transition-State Geometric Variations. From the preceding discussion and a basic model, it is possible to evaluate various changes in transition-state geometry for the reaction of interest by comparing their relative effects on the calculated KIE values. A significant amount of information can be gained by making systematic changes in the basic geometric model, while holding the force field fixed from one model to another. Therefore, in addition to the models presented thus far, numerous other models were created in order to investigate other geometric parameters. The calculated KIE-20 values can be compared directly for geometric changes which have essentially no effect on the temperature dependence. For those changes which do affect the temperature dependence, comparison of values at a single temperature is not diagnostic and the 20–60 differences must be compared. The results of these additional models are summarized in the following paragraphs.

C–Cl Bond Length. When the 20–60 difference (the temperature dependence) is plotted vs. the central carbon–chlorine distance, the curve shows a linear increase over the first 50% increase in C–Cl bond length (20–60 difference at this point is 12.2×10^{-4}) and then begins to show curvature. Beyond a value corresponding to 250% of the C–Cl ground-state value ($20\text{–}60 = 12.9 \times 10^{-4}$), no change is seen with further increase in C–Cl distance. It seems possible, therefore, to correlate the

Table XII. Normalized Eigenvectors[a] of *n*-Butyl Chloride Transition-State Model 12

	r_1	r_2	β_1	β_2	γ_1	γ_2	α	Δ	R	R
ν_1	1.000	1.000					−0.180		−0.103	
ν_2			1.000	1.000	−0.463	−0.463	0.582			
ν_3			−0.166	−0.166	−0.465	−0.465	1.000		0.156	
ν_4					0.472	0.472	−0.887	−0.415	1.000	0.244
ν_L			−0.513	−0.513	−0.109	−0.109	0.542	−0.774	−0.448	1.000
ν_6					−0.189	−0.189	0.193	1.000		0.628
ν_7	1.000	−1.000			−0.162	0.162				
ν_8			1.000	−1.000	0.164	−0.164				
ν_9			−0.124	0.124	1.000	−1.000				

[a] Refer to Figure 1 for notation.

Table XIII. Calculated KIE Values of Model 12 Compared with Measured Values[a]

T, °C	Calcd	Measured	% deviation[c]
0	1.00966	1.00962	0.0040
10	1.00931		
20	1.00898	1.00898	0.0000
30	1.00868		
40	1.00840	1.00841	0.0010
50	1.00815		
60	1.00791	1.00792	0.0010

[a] Reference 35. [b] Value with the nucleophile was calculated to be 1.00898 with a 20–60 difference of 10.5×10^{-4} and a decomposition frequency of -68.19 cm^{-1}. [c] Average deviation = 0.0015%.

temperature dependence by varying the C–Cl bond length in the transition-state model. The prime effects of increasing this length on the calculated frequencies appears to be an increase of both ν_2 and ν_8, the symmetric and asymmetric modes involving angle β, and also an increase in ν_6, the C–C–Cl bending mode.

C–H Bond Length. The variation of the 20–60 difference with C–H bond lengths shows a linear relationship over the limited range of a 5% increase to a 5% decrease over the ground-state value. The magnitude of change in the 20–60 difference is almost twice that of the C–Cl bond changes above, and is in the *opposite* direction, i.e., the 20–60 difference decreases with increasing C–H bond length. These results suggest that, over a limited range, the change in C–H bond length is twice as effective in adjusting the temperature dependence as were changes in the C–Cl bond length. The vibrational analysis shows that an increase in this bond has the effect of decreasing the frequencies of all angular modes which have this bond as one side, i.e., both β modes (ν_2 and ν_8), the γ mode (ν_9), and the α mode (ν_3).

C–C Bond Length. The temperature dependences of models where the C–C bond length is varied are essentially equivalent. The KIE-20 values, therefore, may be compared for these models. The linear decrease in KIE-20 values with increasing C–C bond lengths is reflecting the changes in TDF as this bond increases, because the TIF is essentially constant for these models (1.0036). The TDF values range from 1.00525–1.00530. Although the change is slight, the correlation is definite, and it appears that the TDF can be varied to a limited extent by changing the C–C bond length. The primary effects on the frequencies of increasing this bond appear to be an increase in the γ mode (ν_9) and also in the α mode (ν_3).

Dependence on Angles α and γ. Model 1 assumed no change in angle α (∠H–C–H). Therefore, it was of interest to see what effects an increase in this angle, and consequently, a decrease in angle γ, would produce. The KIE-20 values as a function of angle α (angle γ is equal to $(360 - \alpha)/2$ show a dependence which is linear, as in the C–C bond length case above, but is of opposite direction and its magnitude is only about half as great, i.e., an increase of 10% of α was required to produce the same change in KIE-20 values as a 5% decrease in the C–C bond length. Here, again, this correlation is reflecting the changes in the TDF (1.00527–1.00534). However, this dependence is of slightly *higher* magnitude (but opposite direction) than for the C–C bond case and may be a more effective geometric parameter when adjusting the TDF. There do not appear to be any major effects of changes in these angles on the calculated frequencies.

For the reaction of *n*-butyl chloride with thiophenoxide anion, model 12 and force field 2 are very effective in reproducing the experimental KIE data, as evidenced by the average deviation of 0.0015% as shown in Table XIII. This geometric model indicates that the transition state for this classic SN2 reaction is *not* a trigonal bipyramid, as is commonly used in many theoretical calculations, but it is better described by a more reactant-like configuration which is approximately 85% of the way from the ground-state geometry toward the planar configuration. This is consistent with the crystallographic study of Bürgi,[33] which indicates that only when the leaving group and approaching nucleophile are approximately equidistant from the central atom (corresponding to ca. 20% increase in C–Cl distance) is the transition-state geometry a trigonal bipyramid. The C–Cl bond length of model 12 has been increased only 2% over its ground-state value due to geometric consideration of the temperature dependence.

Importance of the Temperature Dependence. The precise way in which the kinetic isotope effect values vary with temperature for the reaction under study (specified in this work by the 20–60 difference) is considered to be a very important criterion in the evaluation of transition-state models. The comparison of the experimentally measured temperature dependence with that calculated for a specific model gives a reliable measure of the validity of that model. This temperature dependence is, for the most part, determined by the zero point energy factor (ZPE). For example, the change in this factor was ten times greater than that of the EXC term over the experimental range of interest. This term is given by

$$\mathrm{ZPE} = \frac{\exp\left[-\frac{h}{2kT}\sum_{i=1}^{3N-7}(\nu_{1i}^{\ddagger} - \nu_{2i}^{\ddagger})\right]}{\exp\left[-\frac{h}{2kT}\sum_{i=1}^{3N-6}(\nu_{1i} - \nu_{2i})\right]}$$

where both sums are over all real vibrations. The contribution to this term by the denominator will be constant for a given ground-state model. Therefore, the temperature dependence will remain constant for any transition-state model unless the sum of the real isotopic shifts changes from model to model. This is indeed the case for *n*-butyl chloride, as geometric parameters which affect the temperature dependence (e.g., the C–Cl or C–H bond distances) result in sums on the order of 20 times different than parameters which do not affect it.

Predicting the parameters, either geometric or force constants, which will affect the final sum is, unfortunately, virtually impossible.

The analysis of various changes in the temperature dependence shows that it would be possible to match the 20–60 difference with a model drastically different from model 12. For example, a large increase in the C–Cl length, over its ground state value, could be proposed. This would require an equally large increase in the C–H length to compensate for the effect of the C–Cl length on the temperature dependence. The probability of this model choice can be evaluated by observation of the secondary deuterium isotope effects. These values are observed to be close to unity for SN2 reactions;[38] e.g., 1.004 ± 0.007 per α-D for reaction of *p*-methylbenzyl chloride with azide ion.[39] These data, then, suggest that large changes in C–H length are not appropriate. For the *n*-butyl chloride system, represented here by model 12 and force field 2, a value for k_H/k_D of 0.981 is calculated without inclusion of the nucleophile and 0.979 with the nucleophile included. These values are not exactly unity, primarily because the ground-state force field is not totally optimized for reproduction of any observed isotopic shifts due to deuterium substitution. Calculated shifts of ca. 800 cm^{-1} for the C–H stretching modes are slightly smaller than the 900–1000 cm^{-1} normally observed. These calculated results from the proposed model, however, are sufficiently close to unity to suggest that the model does meet the expected secondary deuterium values for this type of reaction. The only other experimental evaluations of the proposed model involve actual measurement of the sulfur isotope effect of the nucleophile and the central carbon KIE. A range of 1.036–1.053 is reported[40] for α-^{13}C KIE values at 0.0 °C. A value of 1.044 is calculated both for the nonplanar model 12 and for the planar model 18. These results indicate (1) that our central model gives a central carbon KIE value within the range appropriate for a SN2 reaction and (2) that central-carbon KIE calculations are not sensitive enough to distinguish between the planar and nonplanar models. Work is in progress to obtain both the sulfur and the central-carbon measurements, but their attainment is not a simple experimental problem. The interpretation of the sulfur measurements will not be unambiguous unless the effect of interaction between the solvent and the charged nucleophile can be separated from the isotope effect arising from the attack of the nucleophile on carbon. Other models which might fit both types of kinetic isotope effects would require either radical changes in several force constants or radical changes in the geometric parameters in order to reproduce the observed temperature dependence. The model studies which we have done so far do not suggest a way that this can be readily accomplished. Therefore, although it may be possible to match the KIE values at various temperatures with a drastically different model, the necessary geometric changes or force constant changes are not obvious.

The Approach of the Nucleophile. Throughout the model studies presented, we have considered the inversion process as arising from the approaching nucleophile. In our five-atom skeletal model we initially included no internal coordinates to describe this approach and, consequently, had no *direct* information available as to nucleophile position in the transition state. In most cases the line of approach of the nucleophile is considered to be colinear with the C–Cl bond, i.e., if the C–Cl bond lies on the positive *z* axis, the nucleophile approaches along the negative *z* axis. This was explicitly implied when using the smooth inversion process discussed earlier. A series of models in which the inversion was skewed, e.g., the β angles decreased faster than the Δ angle, was used briefly in an effort to simulate an off-axis approach. The results, however, were almost identical with the colinear inversion series and this method was deemed too insensitive to draw any conclusions on this matter.

In our six-atom skeletal model, we included additional internal coordinates to describe the position of the nucleophile in conjunction with our central model 12. The necessary geometric parameters and force constants were estimated from various assumed bond-order relationships. Table XIII shows that the KIE-20 value and the temperature dependence were matched equally well by this model 12 with included nucleophile and the much simpler model 12 without the nucleophile. Further calculations showed the geometric conclusions to be identical in either case.

The description of the extent of central carbon–chlorine and central carbon–nucleophile bonding has been approached in several ways in the past. Our method for inclusion of the nucleophile is essentially the same as used by Bron[31] in his calculations on the solvolysis of benzyl bromide. This approach was also used by Sims et al.[8] in model calculations for the SN2 reactions of benzyl chloride. This treatment, based on the bond energy bond order (BEBO) method for a three-atom model of reaction, as derived by Johnston,[41] is primarily applicable to hydrogen-transfer reactions in the gas phase, where the process requires the third body for reaction. In the reactions described by this study, and for any which occur in the solution phase, the unimolecular ionization may be competitive with the nucleophilic displacement, making the bond order approach less applicable. In addition, it is difficult for us to test the validity of these simple bond order–force constant relationships. For our five-atom models, the resulting transition-state force field is necessarily compromised by the influence of the nucleophile and the force constants are not *directly* related to their ground-state values by the transition-state bond orders. Inclusion of the nucleophile does eliminate *some* of this compromise, as evidenced by Table IX, but it is not feasible to determine the *extent* to which this compromise is removed because of the close similarity of the description of the transition state. It is of interest, however, to note the small value of $f(R\text{-}\Phi)$. This indicates that there is very little interaction between the C–Cl and C–S stretching modes in the transition state.

Thornton[42] has developed a simple theory for the prediction of substituent effects on transition-state structure. This theory deduces a change in the transition state by summing the effects of a linear perturbation (change in substituent, nucleophile, leaving group) on each of the fundamental modes. Harris and Kurz[13] have further developed the same idea, including calculations based on a simple electrostatic model. An earlier treatment by Bigeleisen and Wolfsberg[34] considers a three-center reaction where one bond is breaking while another is being formed. The reaction coordinate is given as a modified Slater-type coordinate and a parameter, *P*, is defined such that the square root of *P* determines the relative amount of bond formation to bond extension. An expression is derived for the ratio of decomposition frequencies (TIF) in terms of *P* and the masses of the leaving group, central group, and nucleophile. This derivation assumes a simple relationship between the extent of bonding and the masses of the bonding substituents, and ignores any coupling of modes. We have observed, however, that this coupling is very important in both SN1 and SN2 reactions. A further complication arises in that values for the masses required by this expression are not obvious and our attempts to use the calculated TIF of these models to find an absolute value of *P* are tenuous.

Although these approaches have strong intuitive arguments for their use, they all require more assumptions than one can presently test with the available data. We have chosen, instead, to let the agreement between calculated and measured kinetic isotope effects guide the changes in the ground-state model necessary to produce the transition-state model. In this manner, the effect of the nucleophile on the potential energy of the transition state is necessarily reflected by the degree of ad-

justment in converting the ground-state force field to the transition-state force field. If central-carbon atom isotope effect values and/or nucleophile isotope effects could be simultaneously included in the model calculations, the amount of available information may be further increased and it might be possible to evaluate these other approaches more thoroughly. (This is the point suggested much earlier by Fry.[2]) In particular, it would be most interesting to use this approach to evaluate the predictions of Thornton pertaining to nucleophilic or leaving group substituent effects. We are presently working toward this goal.

Comparison. The eigenvectors of Table XII show the decomposition frequency, ν_L, to be a complex mixture of internal modes. This large amount of mixing is in contrast to our earlier predictions on molecules of low symmetry.[19] The major contribution does come from the C-Cl stretching coordinate, however, and the small isotopic shift in this frequency indicates that the amount of bonding of chlorine to carbon in the transition state is small, but definite.

The earlier studies from these laboratories of the temperature dependence of the *n*-butyl chloride reaction[11] employed the heavy-atom approximation[43] of the Bigeleisen equation for calculating the TDF, assuming that the only isotopically dependent vibration was the C-Cl stretching frequency. The reported value at 20 °C was 1.00451, which is low compared to the value of 1.00525 calculated here for model 12. This is to be expected, however, since several vibrations which are isotopically dependent have been observed for this molecule.

Finally, a comparison of the dependences of KIE results on various geometric parameters between the SN2 case and the SN1 case[19] shows the same general form of dependence on C-CL bond length, except that the SN2 case produces smaller changes in KIE for a given percent change in bond length. The C-C bond changes follow the TIF in the SN1 case, but follow the TDF for the SN2 reaction. The degree of central group planarity in the transition state is related to the TIF in both cases. The SN1 case, however, shows an approximately linear relationship as compared to the parabolic correlation in the SN2 case.

References and Notes

1) This research was supported by grants (MPS 73-08429 and MPS 75-21059) from the National Science Foundation.
(2) A. Fry in "Isotope Effects in Chemical Reactions", C. J. Collins and N. S. Bowman, Ed., Van Nostrand-Reinhold, New York, N.Y., 1970.
(3) L. Melander, "Isotope Effects on Reaction Rates", Ronald Press, New York, N.Y., 1960.
(4) (a) M. Wolfsberg, *Annu. Rev. Phys. Chem.*, **20**, 449 (1969); (b) *Acc. Chem. Res.*, **5**, 225 (1972).
(5) J. W. Hill and A. Fry, *J. Am. Chem. Soc.*, **84**, 2763 (1962).
(6) E. P. Grimsrud and J. W. Taylor, *J. Am. Chem. Soc.*, **92**, 739 (1970).
(7) T. M. Bare, N. B. D. Hershey, H. D. House, and C. G. Swain, *J. Org. Chem.*, **37**, 997 (1972).
(8) L. B. Sims, A. Fry, L. T. Netherton, J. C. Wilson, K. D. Reppond, and S. W. Crook, *J. Am. Chem. Soc.*, **94**, 1364 (1972).
(9) D. G. Graczyk and J. W. Taylor, *J. Am. Chem. Soc.*, **96**, 3255 (1974).
(10) J. Bigeleisen and M. Wolfsberg, *Adv. Chem. Phys.*, **1**, 15 (1958).
(11) C. R. Turnquist, J. W. Taylor, E. P. Grimsrud, and R. C. Williams, *J. Am. Chem. Soc.*, **95**, 4133 (1973).
(12) C. G. Swain and E. R. Thornton, *J. Am. Chem. Soc.*, **84**, 817 (1962).
(13) J. C. Harris and J. L. Kurz, *J. Am. Chem. Soc.*, **92**, 349 (1970).
(14) M. Wolfsberg and M. J. Stern, *Pure Appl. Chem.*, **8**, 225, 325 (1964).
(15) M. J. Stern, W. Spindel, and E. U. Monse, *J. Chem. Phys.*, **48**, 2908 (1968).
(16) W. Spindel, M. J. Stern, and E. U. Monse, *J. Chem. Phys.*, **52**, 2022 (1970).
(17) T. T. S. Huang, W. J. Kass, W. E. Buddenbaum, and P. E. Yankwich, *J. Phys. Chem.*, **72**, 4431 (1968).
(18) J. H. Keller and P. E. Yankwich, *J. Am. Chem. Soc.*, **95**, 7968 (1973).
(19) (a) R. C. Williams and J. W. Taylor, *J. Am. Chem. Soc.*, **95**, 1710 (1973); (b) *Ibid.*, **96**, 3721 (1974).
(20) K. N. Rao, C. J. Humphreys, and D. H. Rank, "Wavelength Standards in the Infrared", Academic Press, New York, N.Y., 1966.
(21) R. C. Williams, Ph.D. Dissertation, University of Wisconsin, 1972.
(22) R. G. Snyder and J. H. Schachtschneider, *J. Mol. Spectrosc.*, **30**, 290 (1969).
(23) F. A. Miller and F. E. Kiviat, *Spectrochim. Acta, Part A*, **25**, 1363 (1969).
(24) See, for example, L. J. Bellamy, "The Infrared Spectra of Complex Molecules", Wiley, New York, N.Y., 1964.
(25) E. B. Wilson, Jr., J. C. Decius, and P. C. Cross, "Molecular Vibrations", McGraw-Hill, New York, N.Y., 1955.
(26) C. N. R. Rao, "Chemical Applications of Infrared Spectroscopy", Academic Press, New York, N.Y., 1963.
(27) T. Ukaji and R. A. Bonham, *J. Am. Chem. Soc.*, **84**, 3627 (1962).
(28) A. B. Dempster and G. Zerbi, *J. Mol. Spectrosc.*, **39**, 1 (1971).
(29) C. G. Opaskar and S. Krimm, *Spectrochim. Acta, Part A*, **23**, 2261 (1967).
(30) For example, B. N. Cyvin and S. J. Cyvin, *Acta Chem. Scand.*, **26**, 3943 (1972).
(31) J. Bron, *Can. J. Chem.*, **52**, 903 (1974).
(32) G. S. Hammond, *J. Am. Chem. Soc.*, 77, 334 (1955).
(33) H. B. Bürgi, *Inorg. Chem.*, **12**, 2321 (1973).
(34) J. Bigeleisen and M. Wolfsberg, *J. Chem. Phys.*, **21**, 1972 (1953).
(35) Because a plot of the logarithm of KIE values vs. inverse temperature is linear over the experimental range of interest (0–60 °C), the data of ref 11 has been analyzed by a least-squares program and values reported here are those taken from the best line.
(36) (a) A. M. Katz and W. H. Saunders, *J. Am. Chem. Soc.*, **91**, 4469 (1969); (b) W. H. Saunders, *Chem. Scr.*, **8**, 27 (1975).
(37) L. Pauling, *J. Am. Chem. Soc.*, **69**, 542 (1947).
(38) V. J. Shiner, Jr., M. W. Rapp, and H. R. Pinnick, *J. Am. Chem. Soc.*, **92**, 232 (1970), and references cited therein.
(39) V. F. Raaen, T. Juhlke, F. J. Brown, and C. J. Collins, *J. Am. Chem. Soc.*, **96**, 5928 (1974).
(40) S. E. Scheppele, *Chem. Rev.*, **72**, 511 (1972).
(41) H. S. Johnston, "Gas Phase Reaction Rate Theory", Ronald Press, New York, N.Y., 1966, pp 339–345.
(42) E. R. Thornton, *J. Amer. Chem. Soc.*, **89**, 2915 (1967).
(43) M. J. Stern and M. Wolfsberg, *J. Pharm. Sci.*, **54**, 849 (1964).